Safety Science 50 (2012) 751–760

Contents lists available at SciVerse ScienceDirect

Safety Science

journal homepage: www.elsevier.com/locate/ssci

Special Issue Article: The First International Symposium on Mine Safety Science and Engineering

# Relationship between EMR and dissipated energy of coal rock mass during cyclic loading process ☆

Dazhao Song *, Enyuan Wang, Jie Liu

*School of Safety Engineering, China University of Mining and Technology, Xuzhou, Jiangsu 221008, China*
*State Key Lab of Coal Resources and Safe Mining, College of Resources and Safety Engineering, Xuzhou, Jiangsu 221008, China*

ARTICLE INFO

*Article history:*
Available online 15 September 2011

*Keywords:*
Coal rock mass
EMR energy
Dissipated energy
Hysteresis loop area
Amplitude

ABSTRACT

Dynamic collapses of deeply mined coal rocks are severe threats to miners. In order to predict the collapses more accurately using electromagnetic radiation (EMR), this paper researched the energy conversion mechanism in the damage process of coal rock mass, analysed its EMR and dissipated energy, and a relationship between which was established using the voltage amplitude of EMR signal and hysteresis loop generated in the loading and unloading cycles as a bridge; then a series of cyclic loading experiments using coal samples of Junde and Xinlu coal mines from Heilongjiang province were carried out, and EMR signal released during these cycles were collected. Results show that during a whole damage process of a sample, the cumulative values of EMR energy and corresponding dissipated energy (hysteresis loop area) well subject to the form of $y = a\ln(x) + b$, whose correlation coefficients are above 0.90, and EMR signals received by different frequency antenna seldom impacted on this relationship; the total EMR energy released from the whole failure process of the samples obtained from adjacent sampling point in same mining area are different to some extent, so are the dissipated energy; compared with cyclic loading for coal rock mass orderly with the peak loads of 5 kN and 10 kN previously, the dissipated energy of direct using that of 15 kN increase 17.8%, and EMR signal is more abundant; EMR energy received in each cycle increase steadily with the improvement of load level, and in a single loading and unloading cycle, sometimes it is very rich in the unloading phase, even more than the loading one.



## 1. Introduction

Numerous investigations showed a relationship between applied stress and EMR emitted from rock material (Hadjicontis and Mavromatou, 1994; Krylov and Nikiforova, 1996; Wang et al., 2005; Lichtenberger, 2006). Results from modellings (O'Keefe and Thiel, 1995; Molchanov and Hayakawa, 1995; Mognaschi, 2002), laboratory experiments (tests) (Cress et al., 1987; Wang and He, 2000; Frid et al., 2005) as well as field observations (Frid, 1997, 2001; He et al., 1999; Liu and He, 2001; Wang et al., 2009a) suggested that small scale fracturing processes are the main source of this EMR. As an important parameter, amplitude (of the voltage) of EMR has been aroused wide attention. Frid et al. (1999) and Rabinovitch et al. (2001, 2007), analyzing EMR amplitude changes induced by rock compression, showed a similarity in the fractal nature of the processes controlling earthquakes and those of EMR induced by rock fracture, and amplitude of EMR pulses was the square root of the electromagnetic energy recorded; the EMR amplitude was also a function of the crack area; they carefully verified the correlation between crack sizes and pulse parameters, and built a EMR model showing that crack velocity was proportional to the EMR amplitude. Mori et al. (2004), by cyclic loading tests, found the plots of the signal amplitude of EMR was a function of the elapsed time of loading; the EMR signal was accompanied with the generation of AE signal, and there was a positive correlation between the amplitude of EMR and AE signal, which was useful for estimating the rock in situ stress. Kurlenya et al. (1991) researched the relationship between frequency and amplitude of EMR, found the maximum spectral amplitude of EMR at the time of growth of the main crack was shifted toward higher frequencies. Xiao et al. (2006) researched the energy

☆ The First International Symposium on Mine Safety Science and Engineering (ISMSSE2011) will be held in Beijing on October 26–29, 2011. The symposium is authorized by the State Administration of Work Safety and is sponsored by China Academy of Safety Science & Technology (CASST), China University of Mining & Technology (Beijing) (CUMTB), Datong Coal Mine Group, McGill University (Canada) and University of Wollongong (Australia) with participation from several other universities from round the world, research institutes, professional associations and large enterprises. The topics will focus on mines safety field: theory on mine safety science and engineering technology, coal mine safety science & engineering technology, metal and nonmetal mines safety science & engineering technology, petroleum and natural gas exploitation safety science & engineering technology, mine safety management and safety standardization science & technology, occupational health and safety in mine, emergent rescue engineering technology in mine, etc.

* Corresponding author at: School of Safety Engineering, China University of Mining and Technology, Xuzhou, Jiangsu 221008, China. Tel.: +86 158 621 714 77.
*E-mail address:* song.dz@cumt.edu.cn (D. Song).

0925-7535/$ - see front matter © 2011 Elsevier Ltd. All rights reserved.
doi:10.1016/j.ssci.2011.08.039

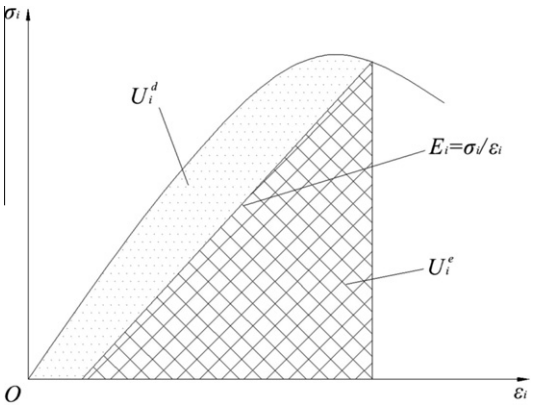


**Fig. 1.** Relationship between dissipated energy and releasable strain energy of rock mass unit.

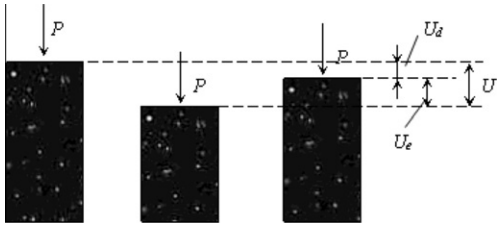


**Fig. 2.** Coal load diagram.

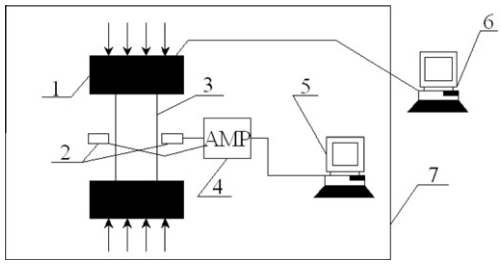


**Fig. 3.** EMR test system. 1 – Compression testing machine, 2 – magnetic loop antennae, 3 – sample, 4 – preamplifiers, 5 – data acquisition and processing system, 6 – load control system, 7 – electromagnetic shielding room.

transformation between EMR signal and stress in the course of deformation and failure of coal rock, and found the changing curve between EMR and mechanical energy was consistent with the relation curve between stress and strain, which conformed to thrice multinomial approximately. Moreover, an increase of elasticity, strength, and loading rate enhanced the EMR amplitude (Wang et al., 2009b).

EMR monitoring and early warning techniques have been widely used in coal mines in China. As a kind of soft rock, coal has some similar features with common rocks. Meanwhile, as a state variable, using energy to solve problems not only can greatly simplify the analysis of intermediate process, but also take more holistic and comprehensive account of various factors. To some extent, studying complex rock mechanics problems underground from the energy point of view is more suitable. So the aim of the paper is to experimental study the relationship between EMR and dissipated energy released from coal loaded, using the parameter—amplitude of EMR, and to try to explore new ideas for early warning coal bumps using EMR.

## 2. Energy analysis of damage and failure of coal rock mass

As a kind of non-homogeneous multi-phase composite material, a large number of micro-cracks and voids, and some other natural defects are formed in coal rock mass in the long-term tectonic movements. Subjected to external forces, coal rock mass will experience four phases: the micro-crack closure phase, the elastic deformation phase, the micro-defects evolution and extension phase, and the destruction phase. In this process, coal rock mass always exchange energy with the external: the external mechanical energy turns into strain energy, thermal energy stores for internal energy. Then strain energy turns into its own plastic strain energy, surface energy, etc., meanwhile, the mass will release energy to the external in the form of EMR, AE, etc. (Mikhalyuk and Zakharov, 1996; Sujathal and Chandra-Kishen, 2003; Xie et al., 2005).

Xie (1998) reveals under external forces, two mechanisms—"strain hardening" and "strain softening" can be produced inside the coal rock mass, which compete with and influence each other, and jointly determine its macroscopic properties. The deformation and fracture of coal rock mass is relevant to its internal energy changes, including energy accumulation, release and dissipation. That is, assuming there is no heat exchange between coal rock mass and the external, the energy accumulated will be self-organized by elastic energy release and plastic energy dissipation:

$$U = U_e + U_d \tag{1}$$

where $U$ is energy variation during the self-organizing process; $U_e$ is elastic strain energy that can be released, while $U_d$ is dissipated energy.

Which, $U_d$ can be expressed as follows:

$$U_d = f(U_p, U_s, U_v, U_r, U_b, U_x) \tag{2}$$

where $f$ is a general nonlinear function of $U_p$, $U_s$, $U_v$, $U_r$, $U_b$ and $U_x$. $U_p$ is plastic energy caused by plastic deformation, $U_s$ is surface energy consumed by the formation of new surfaces, $U_v$ is kinetic energy while collapse, $U_r$ is all sorts of radiation energy, $U_b$ is biological activity energy, and $U_x$ is other forms of energy has not been found.

Xie et al. (2008) expresses the relationship between energy of rock mass unit as Fig. 1. Which, $U_i^d$ represents the energy consumed by rock unit during the formation of damage and plastic deformation process, corresponding to the dissipated energy $U_d$ in Eq. (1). The variation of $U_d$ meets the second law of thermodynamics, that is, the changes of its internal state are consistent with the trend of entropy increase. $U_i^e$ represents the storage releasable strain energy, corresponding to $U_e$ in Eq. (1). This part is directly related to the unloading elastic modulus and Poisson's ratio. From the view of thermodynamics, the energy dissipation is unidirectional and irreversible, while the energy release is a two-way process, which is reversible as long as some certain conditions.

**Fig. 4.** Physical picture of experimental system.

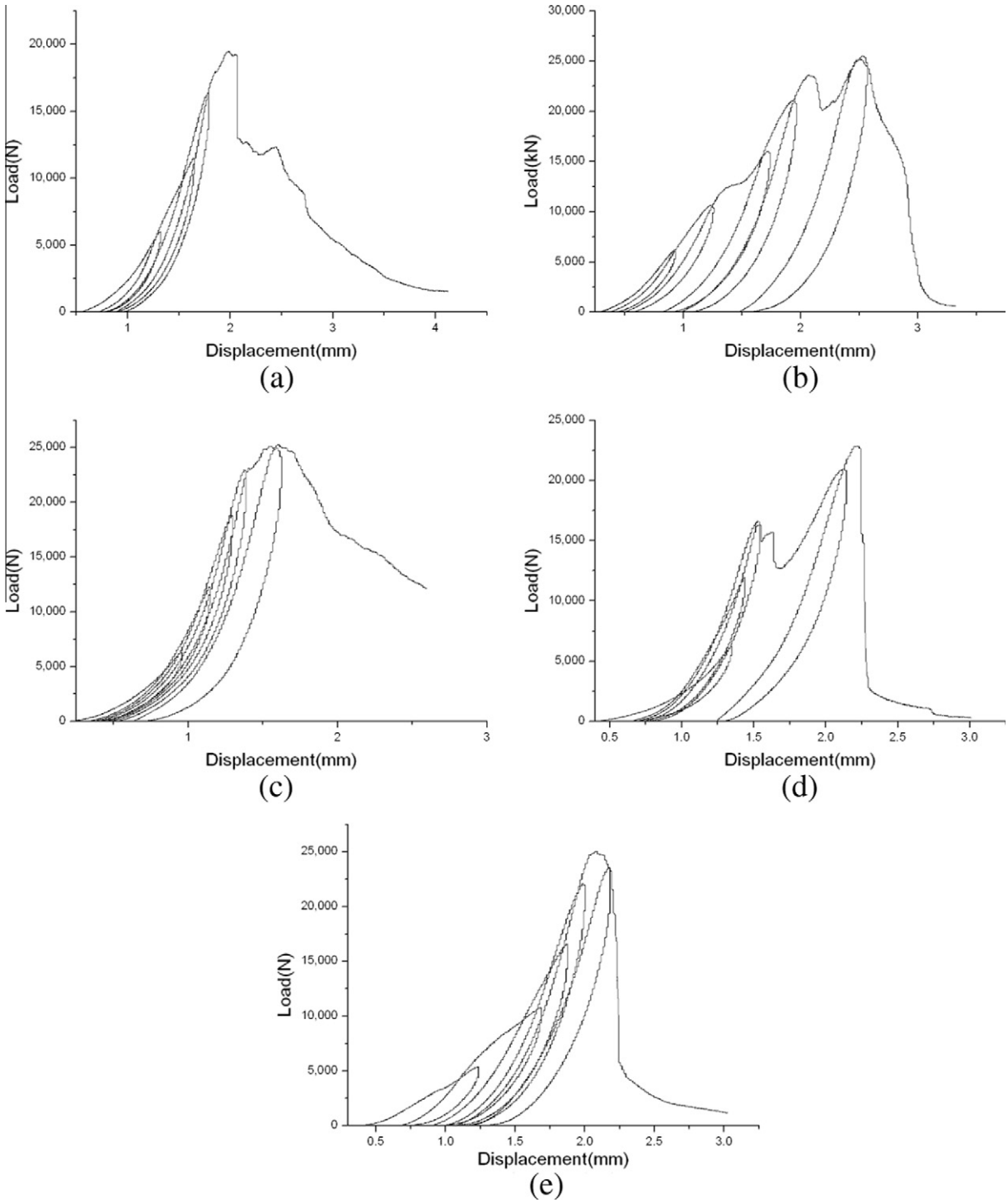


**Fig. 5.** Load–displacement curves of coal samples 1–5# of Junde coal mine.

During the last few decades, the mechanism of EMR was deeply studied. Once a material is brought close to its limit of fracture strength and to frictional sliding, fractures will be formed, and the EMR pulses emitted. EMR may start during crystal deformation prior to and during the nucleation phase of cracks. Due to the cracking of bonds between ions, a polarization occurs at the cracks. Any relative movement of the polarized crack walls gives rise to the emission of EMR (O'Keefe et al., 2000; Frid and Vozoff, 2005; Greiling and Obermeyer, 2010). Although the formers illustrated the mechanism of EMR from different angles, one thing has been a broad consensus, namely, the generation of EMR are closely related to micro-fracture and cracks in coal rock mass loaded. According to the analysis above, the shaded areas expressed dissipated energy in Fig. 1 and the generation of EMR signals have some intrinsic links.

## 3. EMR and dissipated energy in the failure process of coal rock mass loaded

### 3.1. EMR energy

Under laboratory conditions, we commonly use EMR instruments or acoustic–electric dynamic acquisition system to test

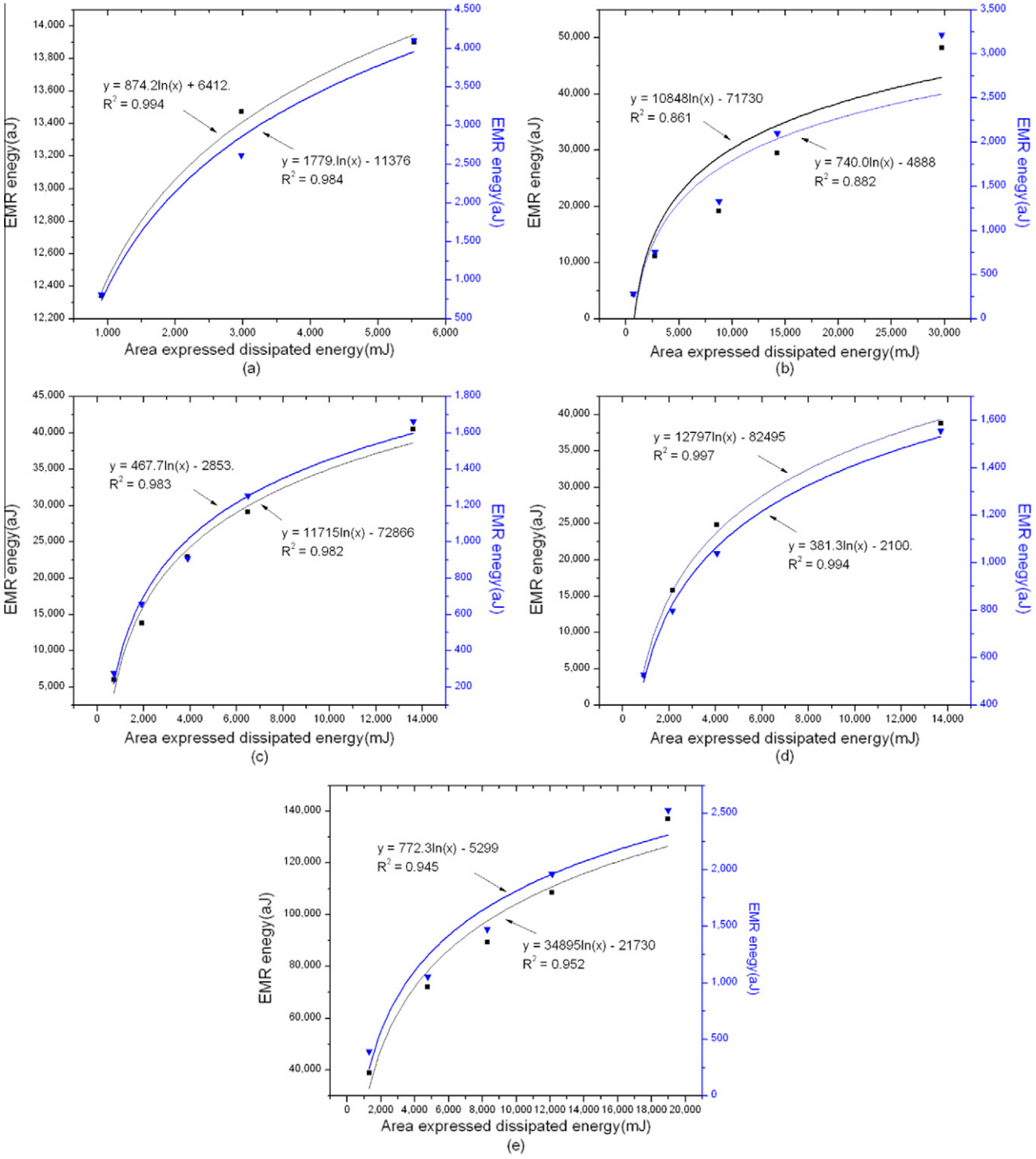


**Fig. 6.** Fitting curves of EMR and dissipated energy for coal samples 1–5# of Junde coal mine. ■ and ▼ present fitting curves between EMR signals and corresponding hysteresis loop areas received by antennae with frequencies of 300 kHz and 50 kHz, respectively; and the units aJ and mJ are $1 \times 10^{-18}$ J and $1 \times 10^{-3}$ J, respectively, hereinafter the same.

EMR signals generated from coal rock mass loaded. This cannot get the actual electric and magnetic fields strength of the electromagnetic field caused by loading coal rock mass, but just the voltage amplitude of the induced voltage or analog signals. For an EMR device, its energy analysis is mainly through the integration of the output transient signal (voltage amplitude), that is,

$$W = \int_0^\infty U(t)I(t)dt \tag{3}$$

where $U(t)$ and $I(t)$ are transient voltage (V) and current (A), respectively.

The actual processing is commonly to discrete Eq. (3):

$$W = \sum_0^n U_i I_i \Delta t \tag{4}$$

where $U_i$ and $I_i$ are voltage and current of sampling points, respectively. $\Delta t$ is the interval of sampling points, and $n$ is the number of sample points.

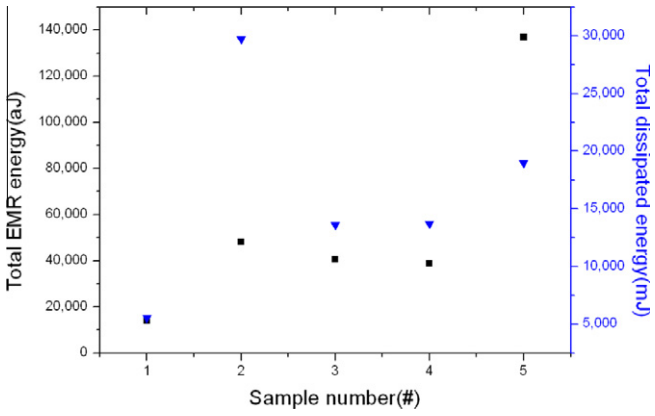


**Fig. 7.** Total energy values of the five samples of Junde mine. ■ and ▼ are total EMR energy received by antenna with frequency of 300 kHz and corresponding dissipated energy, respectively.

**Table 1**
Comparison of dissipated energy.

| Peak load (kN) | Option 1 | Option 2 | | | |
|---|---|---|---|---|---|
| | Average values of dissipated energy of the five samples (mJ) | 1# (mJ) | 2# (mJ) | 3# (mJ) | Average (mJ) |
| 5 | 906.62 | 1035.79 | 793.92 | 736.18 | 855.30 |
| 15 | 2396.89 | 2765.93 | 3922.74 | 1783.94 | 2824.20 |

Eq. (4) is the EMR energy collected in laboratory.

### 3.2. Dissipated energy

In uniaxial compression process, the energy accumulated in coal rock mass is provided by press for power, which has two loading modes: displacement and force load. Adopting the former one, and let the instantaneous force of the loading surface be $P(t)$, the power supplied by press when loading surface moves from 0 to $x$ is

$$W_k = \int_0^x P(t)dt \tag{5}$$

By the analysis above, during the loading process in Fig. 2, the part cannot be recovered represents dissipated energy $U_d$, which is the main source of EMR signal, and corresponds to $U_i^d$ in Fig. 1, i.e., the hysteresis loop area of the first cycle. From Fig. 2, we can also deduce that during the first cycle, the cumulative number of EMR energy $E_1$ is clearly relevant to $U_{d1}$, the hysteresis loop area of this cycle; Accordingly, the first two cycles of cumulative number of EMR energy $E_{1+2}$ is related to that of $U_{d1} + U_{d2}$, i.e., it corresponds to the hysteresis loop areas of the first two cycles.

In this way, the relationship between EMR and dissipated energy is established from the experimental point of view. The following is to analyse the quantitative relationship between the two in the cyclic loading process.

## 4. Experiments

### 4.1. Sampling and methodology

#### 4.1.1. Samples

The samples were taken from the Junde and Xinlu coal mines, Heilongjiang province. We first got big coal mass in mines, and directly processed them into standard cylinder samples of $\Phi 50 \times 100$ mm, with surface flatness error of both ends less than 0.02 mm; then rigorously selected them: (1) eliminate specimens with significant damage and visible cracks on their surfaces; (2) eliminate specimens with the size and flatness do not meet the requirements. To ensure the comparability of experiments results, coal samples in a same group were obtained by densely drilling on the same surface of a coal mass.

#### 4.1.2. Equipments

EMR test system is the core system shown in Fig. 3, composed of the loading system, the data acquisition system, and the electromagnetic shielding system. The physical system is shown in Fig. 4.

(1) Loading system: servo-controlled mechanical test equipment YAW4306, with maximum load capacity $3.0 \times 10^3$ kN; resolution of test force showed (FS) 1/300,000 with relative error 1%; loading speed 600–60,000 N/s with accuracy of ±1%. YAW4306 has two control modes: displacement and force load, which can be used to uniaxial compression and tension, cyclic loading and creep tests, etc.
(2) Data acquisition system: PCI-2 AE System manufactured by PAC (Physical Acoustic Corporation), which has a board with 18-bit A/D conversion scheme, eight digital I/O, and two complete high-speed channels of real time data acquisition, with real time feature extraction, waveform processing and transfer. Its frequency response is 3 kHz to 3 MHz (at −3 dB points).
(3) Electromagnetic shielding system: electromagnetic shielding room GP6, with the effectiveness as follows: 14 kHz ⩾ 80 dB, 100 kHz ⩾ 100 dB, 300 kHz ⩾ 110 dB, 50 MHz to 1 GHz ⩾ 110 dB.

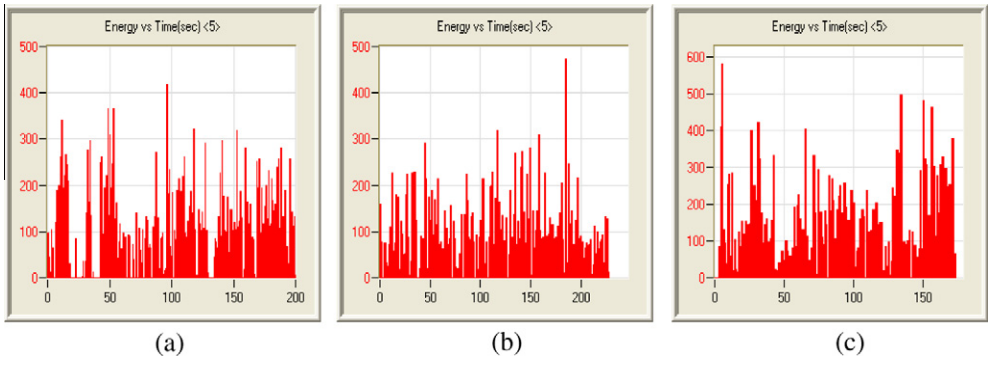


**Fig. 8.** EMR energy released in the cycle with peak load of 5 kN in Option 2. a, b, and c correspond to samples 1#, 2# and 3#, respectively.

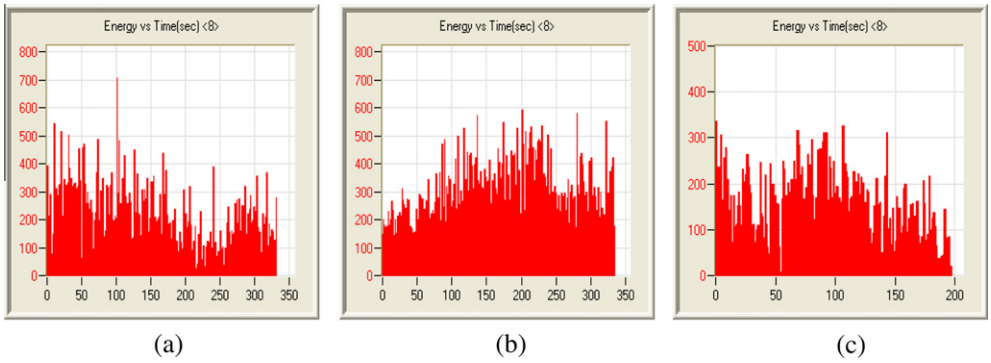


**Fig. 9.** EMR energy released in the cycle with peak load of 15 kN in Option 2. a, b, and c correspond to samples 1#, 2# and 3#, respectively.

**Table 2**
Comparison of EMR energy between the two options.

| Peak load (kN) | Option 1 | Option 2 | | | |
|---|---|---|---|---|---|
| | Average values of total EMR energy of the five samples (aJ) | 1# (aJ) | 2# (aJ) | 3# (aJ) | Average (aJ) |
| 5 | 8773 | 24,059 | 19,006 | 25,374 | 22,813 |
| 15 | 13,159 | 56,762 | 91,753 | 29,903 | 59,473 |

*4.1.3. Methodology*

Option 1: (1) Five samples of Junde coal mine were selected according to Section 4.1.1 and numbered (1#, 2#, 3#, 4#, 5#). (2) Each one was under uniaxial cyclic loading, displacement control mode was used with the speed of 0.1 mm/min. Once the load value was reaching to 5 kN, unload it with the same speed. After the value was to 0, maintain no-load state 90 s (fully eliminated its impact to the next cycle). The first cycle was completed and continued to load. 10 kN, 15 kN, 20 kN, and 25 kN were looked as peak values of the following four cycles. After completion of the whole five cycles, the sample was loaded to failure with the speed of 0.1 mm/min. In the whole process, we adopted two channels (I, II) to acquisite EMR signals, the sensor resonance frequencies were 50 kHz, 57 dB and 300 kHz, 55 dB, respectively.

Option 2: (1) Six samples of Junde coal mine were selected and randomly divided into two groups (a, b), and samples in each group were numbered (1#, 2#, 3#). (2) Each sample was carried out just one loading and unloading cycle, the peak value of group a and b were 5 kN and 15 kN, respectively. In the entire process, EMR signals were recorded.

Do the experiments using samples of Xinlu coal mine as described above.

*4.2. Experimental results and analysis*

*4.2.1. Relationship between EMR and dissipated energy*

*4.2.1.1. Comparison of five cycles of same samples.* From Figs. 5 and 6, the cumulative EMR and corresponding dissipated energy (hysteresis loop area) well subject to the form of $y = a \ln(x) + b$. (The samples of Xinlu mine show the similar law, details please refer to the Appendix.)

This is relevant to two aspects: hysteresis loop area and EMR signal. From the former point of view, numerous research have divided the macroscopic deformation and failure of coal rock mass into four phases (Medhursta and Brownb, 1998): phase I, the compaction phase; phase II, the apparent linear elastic deformation phase; phase III, the accelerated nonelastic deformation phase; and phase IV, the rupture and development phase. Early in the loading process, with relatively intact internal structure, coal rock mass has strong capacity of elastic recovery and resisting external load. Most energy input this time can be stored in the form of elastic energy, which can recover when the load decreases, leading to the hysteresis loop area small in this phase; in the later loading phase, the internal structure of the samples are gradually destructed, making the capacity of bearing external load and storing elastic energy reduce. This time, the work on samples by external load prefer to release as dissipated energy, which leads to weak elastic recovery capacity when external load decreases, making the hysteresis loop area increase. From EMR signals, all the complete cycles are in the former three phases, in which the characteristics of EMR signals have been widely studied (Wang et al., 2009b; Koktavy et al., 2004). In the compaction phase, as almost all

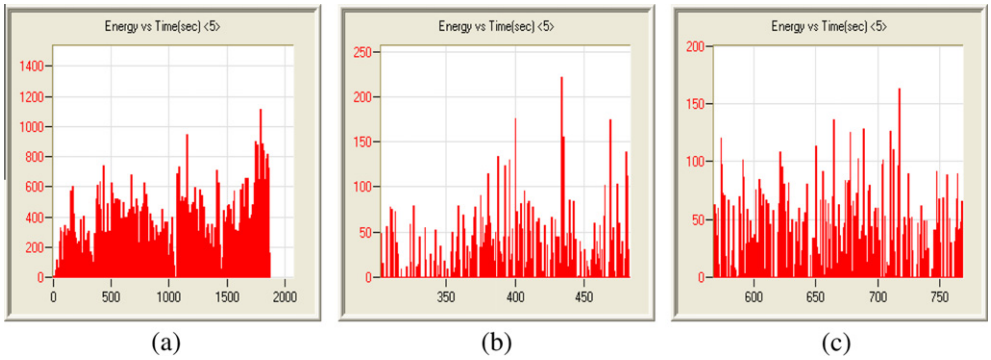


**Fig. 10.** EMR energy of coal sample 3# of Junde mine according to Option 1. (a) is energy–time graph in the whole process, (b and c) are the complete curves of the second and third cycle, respectively.

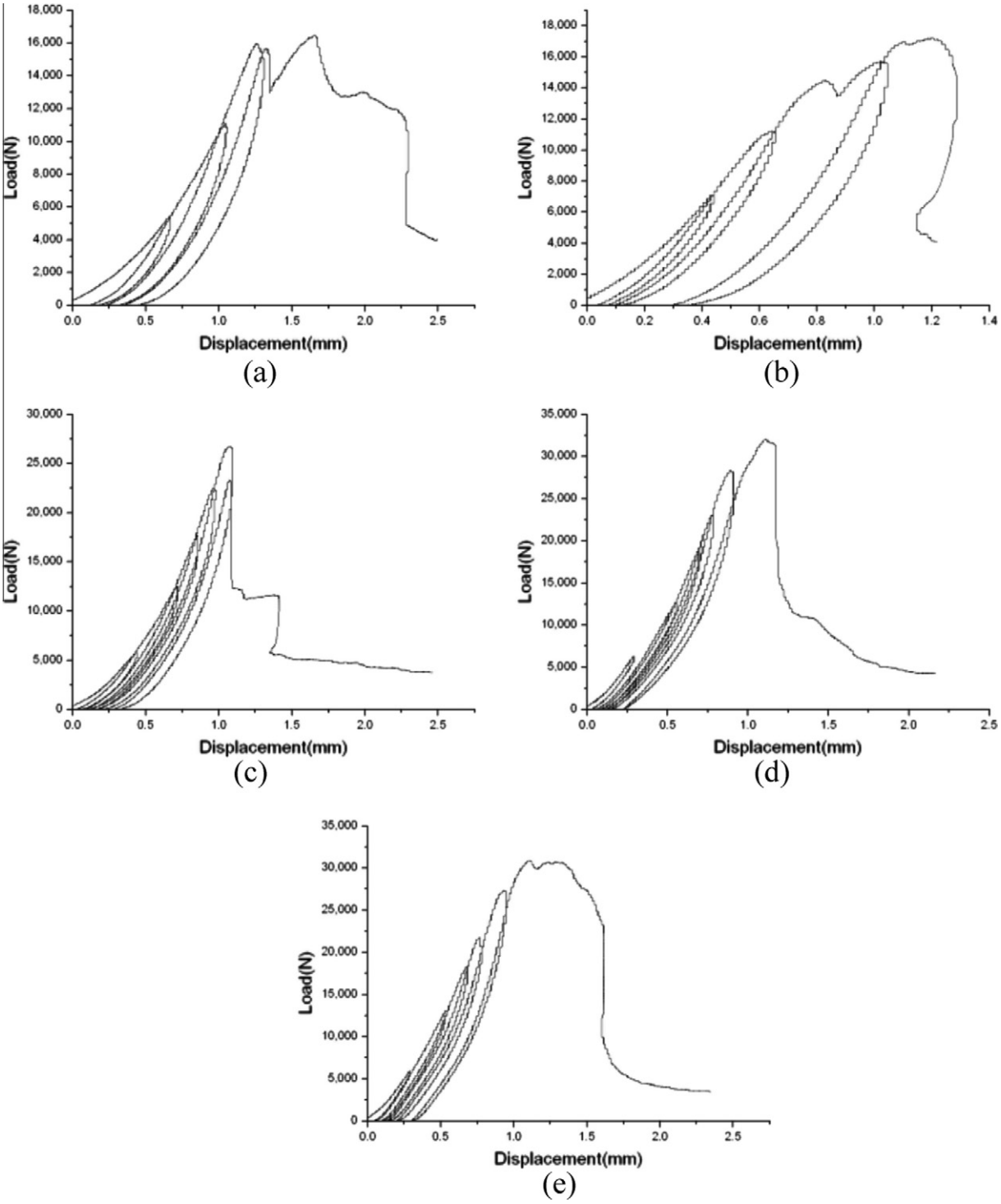


**Fig. A1.** Load–displacement curves of coal samples 1–5# of Xinlu coal mine.

original defects in coal rock mass are to be deformed and micro-fracture, which can produce EMR signals, the cumulative of which at this phase is relatively large, and increase at the beginning and then decrease. In the apparent linear elastic deformation phase, the generation of EMR in microenvironment is episodic rather than continuous. Only the deformation energy in coal can accumulate high enough to cause micro-cracks and generate EMR. By contrast, the macro-EMR signals increase continuously in a nearly linear mode. This is a relatively stable phase. In the accelerated nonelastic deformation phase, large amounts of elastic–plastic energies are accumulated in coal rock mass, resulting in sharply increased EMR counts.

By the analysis above, we believe that with the peak load gradually increases during cyclic loading, the change rate of hysteresis loop area become greater than that of EMR signals, resulting in the phenomenon above.

We also find that signals received by antennae with different frequencies subject to this relationship, and $R^2$ of the fitting equations for a same sample are close, only the values of the two coefficients $a$ and $b$ are different, which results from different

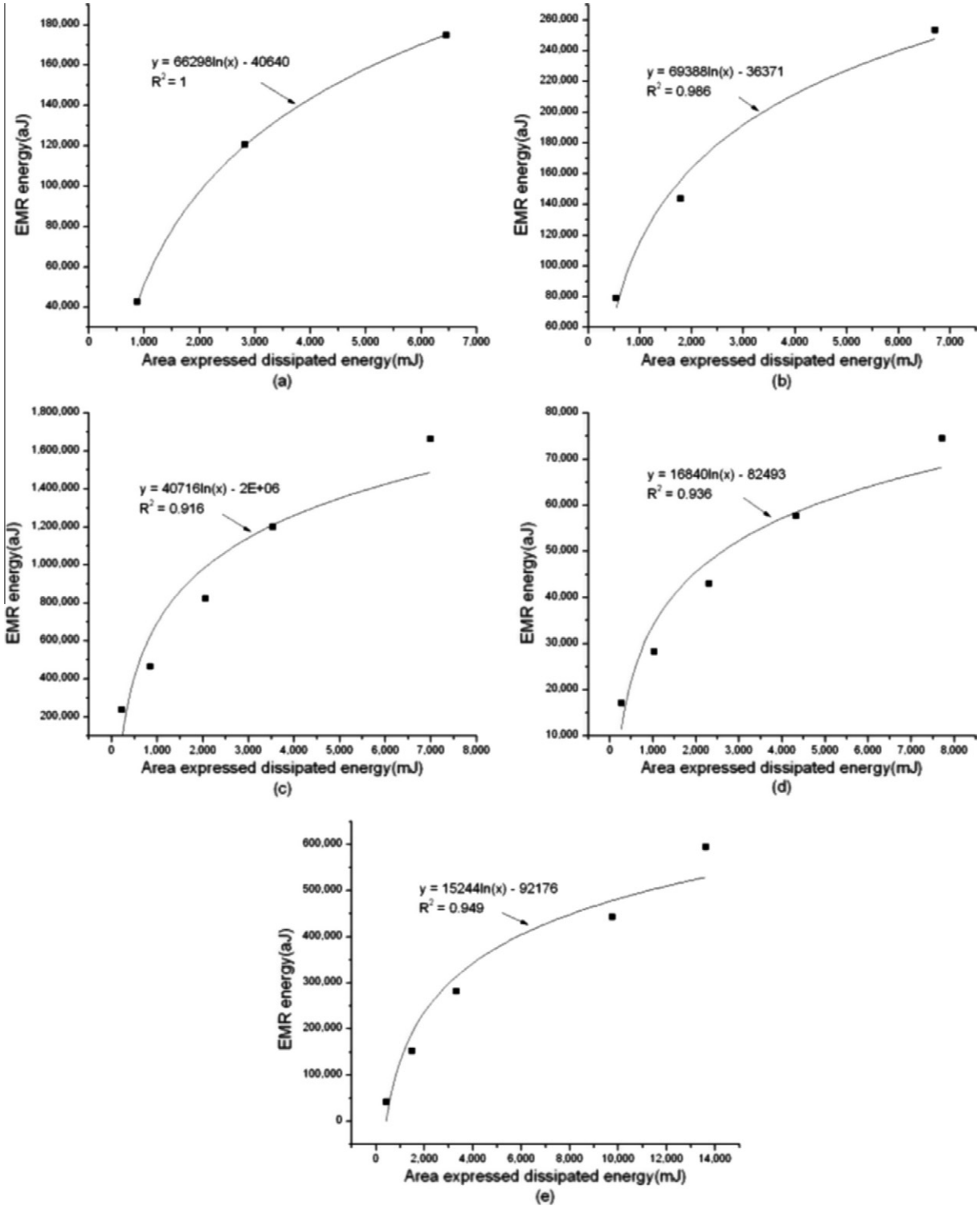


**Fig. A2.** Fitting curves of EMR and dissipated energy for coal samples 1–5# of Xinlu coal mine. EMR signals were received by antenna with frequency of 300 kHz.

frequency points of the two antennae. As the samples of Jude mine are relatively hard, signals of 300 kHz receiver are more abundant. It can be seen that, EMR signals received by different frequency antennae seldomly impacted on this relationship.

Fig. 7 shows both total EMR and dissipated energy are different in the whole cyclic loading process before the complete destruction of the samples. Such as samples 2#, 3# and 4#, whose total EMR energy are between 40,000 and 60,000 aJ, and sample 1# is about 20,000 aJ, the discrepancy of which are insignificant, but the value of the sample 5# is more than 130,000 aJ; meanwhile, the values of the dissipated energy of the five samples have significant differences: the values of samples 1#, 3#, 4# and 5# are less than 20,000 mJ, while the sample 2# is close to 140,000 aJ. For these special points, of course we can look them as singular values, but we have reason to believe these results from the more discrete of coal's internal structure than normal rocks, and can be

attributed to the internal structure of coal. Different loading and unloading paths of the five samples in Fig. 5 can illustrate this from one side.

*4.2.1.2. Comparison of single cycle between the two options.* Table 1 shows the results comparison between the two options according to Section 4.1.3.

From Table 1, with the peak load of 5 kN (as the first cycle in Option 1), the average values of dissipated energy obtained by the two options are 855.30 and 906.62 mJ, respectively, showing a little discrepancy; if the peak load is 15 kN, the value obtained by Option 2 reaches 2824.20 mJ, 17.8% more than the result according to Option 1.

This is because, compared with Option 2, during Option 1, two cycles with peak loads of 5 kN and 10 kN had been orderly carried out before the cycle with peak load of 15 kN, which no doubt caused considerable damage for the samples. Due to the Kaiser effect, this is bound to reduce the damage and fracture during the third cycle, resulting in decrease of hysteretic loop areas and reduction of energy dissipation. While for both the two options, the cycle with peak load of 5 kN is essentially the same, all the samples are in good conditions before loading, therefore, the values of dissipated energy are not very different.

From Figs. 8, 9 and Table 2, the average value of total EMR energy released in the cycle with peak load of 5 kN according to Option 2 is about 2.6 times more than that of Option 1, while that of 15 kN increase 4.5 times, the increment of which is significantly larger than the former one. We believe that this is also relevant to the previous cyclic loading process with peak load of 5 kN and 10 kN, which damage the internal structure of the samples to some extent.

*4.2.2. Comparison of EMR energy of loading and unloading phase in a single cycle*

From Fig. 10a, EMR signal generally improves steadily with the improvement of load level.

Frid (2000) shows that: coal, compared with general rocks, is soft, but can generate EMR in loading process, and at main rupture moment, there can be a strong EMR generated. Through the whole loading process, the EMR intensity increases with the load level improve. For same coal samples, the EMR intensity is good positive correlation with their physical strength, that is, the greater the strength, the greater the intensity of EMR.

The curve in Fig. 10a can be easily divided into five obvious peaks, corresponding to the five cycles. In each cycle, the signal during unloading phase are so rich that even more than that of the loading phase, such as (b) and (c).

From Frid and Vozoff (2005), fractures of the order of 1–2 cm is the main source of measured EMR, which mainly develop along the interfaces between the particles. Compaction can make microcracks spread and crack surfaces slide and rub, leading to the production of free charges and making them proliferate and migrate from high concentration regions (compressed regions) to low concentration regions (low-stress area or stretching regions). But meanwhile, the compressive stress will limit free charges in structures of smaller scales to a certain extent, i.e., at crack tips. When a sample begins to unload, on the one hand, the shear tensile stress can be generated at crack tip, on the other hand, stress relaxation can provide enough movement spaces for free charges, enable their freedom of movement. We think this is the main reason why EMR signal is so rich in unloading phase. In our experiment, the phenomenon that the signal was suddenly increasing once the unloading phase began occurred several times.

## 5. Conclusions

In the failure process, coal rock mass always exchanges energy with the outside. Ignoring the heat exchange, the energy generated by external forces are to self-organize and adjust by the release of elastic energy and dissipation of dissipated energy; the hysteresis loop area generated in cyclic loading process of coal rock mass can be used to express dissipated energy, and the integral of transient signal (voltage amplitude) of EMR can be looked as EMR energy; combining the mechanism of EMR, we established a relationship between EMR and dissipated energy in the failure process of coal rock mass.

The cumulative values of EMR energy and corresponding dissipated energy (hysteresis loop area) for coal samples of Junde and Xinlu coal mine well subject to the form of $y = a \ln(x) + b$, whose correlation coefficients are above 0.90, and EMR signals received by different frequency antennae seldomly impacted on this relationship; the total EMR energy released from the whole process of coal samples obtained from adjacent sampling point in same mining area are different to some extent, so are the dissipated energy; compared with cyclic loading for coal rock mass orderly with peak loads of 5 kN and 10 kN previously, the dissipated energy of directly using that of 15 kN increase 17.8%, and EMR signal is more abundant; the EMR signal increases steadily with the improvement of load level, and in a single cycle, sometimes it is very rich during unloading phase, even more than loading one.

## Acknowledgements

This work is supported by A Foundation for the Author of National Excellent Doctoral Dissertation of PR China (201055) and the Independent Research Project of State Key Lab of Coal Resources and Safe Mining (CUMT) (SKLCRSM09X01).

## Appendix A.

See Figs. A1 and A2.

## References

Cress, G., Brady, B., Rowell, G., 1987. Sources of electromagnetic radiation from fracture of rock samples in laboratory. Geophysical Research Letters 14 (4), 331–334.

Frid, V., 1997. Electromagnetic radiation method for rock and gas outburst forecast. Journal of Applied Geophysics 38 (2), 97–104.

Frid, V., 2000. Electromagnetic radiation method water-infusion control in rockburst-prone strata. Journal of Applied Geophysics 43 (1), 5–13.

Frid, V., 2001. Calculation of electromagnetic radiation criterion for rockburst hazard forecast in coal mines. Pure and Applied Geophysics 158 (5–6), 931–944.

Frid, V., Vozoff, K., 2005. Electromagnetic radiation induced by mining rock failure. International Journal of Coal Geology 64 (1–2), 57–65.

Frid, V., Rabinovitch, A., Bahat, D., 1999. Electromagnetic radiation associated with induced triaxial fracture in granite. Philosophical Magazine Letters 79 (2), 79–84.

Frid, V., Bahat, D., Rabinovitch, A., 2005. Analysis of en échelon/hackle fringes and longitudinal splits in twist failed glass samples by means of fractography and electromagnetic radiation. Journal of Structural Geology 27, 145–159.

Greiling, R.O., Obermeyer, H., 2010. Natural electromagnetic radiation (EMR) and its application in structural geology and neotectonics. Journal of the Geological Society of India 75 (1), 278–288.

Hadjicontis, V., Mavromatou, C., 1994. Transient electric signals prior to rock failure under uniaxial stress. Geophysical Research Letters 21 (16), 1687–1690.

He, X.Q., Wang, E.Y., Liu, Z.T., 1999. The general characteristics of electromagnetic radiation during coal fraction and its application in outburst prediction. In: Proceedings of 8th US Mine Ventilation Symposium. University of Missiouri-Rola Press, Rolla, Missouri, pp. 81–84.

Koktavy, P., Pavelka, J., Sikula, J., 2004. Characterization of acoustic and electromagnetic emission sources. Measurement Science and Technology 15 (5), 973–977.

Krylov, S.M., Nikiforova, N.N., 1996. On ultralow frequency electromagnetic emission from an active geological medium. Physics of the Solid Earth 31 (6), 499–512.

Kurlenya, M.V., Yakovitskaya, G.E., Kulakov, G.I., 1991. Phases in the fracturing process based on EME studies. Rock Breaking.

Lichtenberger, M., 2006. Underground measurements of electromagnetic radiation related to stress-induced fractures in the Odenwald Mountains. Pure and Applied Geophysics 163 (8), 1661–1677.

Liu, M.J., He, X.Q., 2001. Electromagnetic response of outburst-prone coal. International Journal of Coal Geology 45 (2–3), 155–162.

Medhursta, T.P., Brownb, E.T., 1998. A study of the mechanical behaviour of coal for pillar design. International Journal of Rock Mechanics and Mining Sciences 35 (8), 1087–1105.

Mikhalyuk, A.V., Zakharov, V.V., 1996. Dissipation of dynamicloading energy in quasi-elastic deformation processes in rocks. Journal of Applied Mechanics and Technical Physics 38 (2), 312–318.

Mognaschi, E.R., 2002. On the possible origin, propagation and detectability of electromagnetic precursors of earthquakes. Atti Ticinensi di Scienze della Terra 43, 111–118.

Molchanov, O.A., Hayakawa, M., 1995. Generation of ULF electromagnetic emissions by micro fracturing. Geophysical Research Letters 22 (22), 3091–3094.

Mori, Y., Obata, Y., Pavelka, J., Sikula, J., Lokajicek, T., 2004. AE Kaiser effect and electromagnetic emission in the deformation of rock sample. In: DGZfP-Proceedings BB 90-CD, pp. 157–165.

O'Keefe, S.G., Thiel, S.V., 1995. A mechanism for the production of electromagnetic radiation during fracture of brittle materials. Physics of the Earth and Planetary Interiors 89 (1–2), 127–135.

O'Keefe, S.G., Thiel, D.V., Davey, N.P., 2000. Fracture induced electromagnetic emissions in the mining industry. International Journal of Applied Electromagnetics and mechanics 12 (3–4), 203–209.

Rabinovitch, A., Frid, V., Bahat, D., 2001. Gutenberg–Richter-type relation for laboratory fracture induced electromagnetic radiation. Physical Review 65, 011401–011404.

Rabinovitch, A., Frid, V., Bahat, D., 2007. Surface oscillations—a possible source of fracture induced electromagnetic radiation. Tectonophysics 431 (1–4), 15–21.

Sujathal, V., Chandra-Kishen, J.M., 2003. Energy release rate due to friction at bimaterial interface in dams. Journal of Engineering Mechanics 129 (7), 793–800.

Wang, E.Y., He, X.Q., 2000. An experimental study of the electromagnetic emission during the deformation and fracture of coal or rock. Chinese Journal of Geophysics 43 (1), 131–137 (in Chinese).

Wang, E.Y., He, X.Q., Dou, L.M., Zhou, S.N., Liu, Z.T., 2005. Electromagnetic radiation characteristics of coal and rocks during excavation in coal mine and their application. Chinese Journal of Geophysics 48 (1), 216–221 (in Chinese).

Wang, E.Y., Liu, X.F., Zhao, E.L., Liu, Z.T., 2009a. Prediction and control of rock burst of coal seam contacting gas in deep mining. Journal of Coal Science and Engineering 15 (2), 152–156 (in Chinese).

Wang, E.Y., He, X.Q., Li, Z.H., Zhao, E.L., 2009b. Electromagnetic Radiation Technology and Application of Coal or Rock. Science Press Beijing (in Chinese).

Xiao, H.F., He, X.Q., Wang, E.Y., 2006. Research on transition law between EME and energy during deformation and fracture of coal or rock under compression. Rock and Soil Mechanics 27 (7), 1097–1100 (in Chinese).

Xie, H.P., 1998. Damage Mechanics of Rocks and Concrete. China University of Mining and Technology Press Xuzhou (in Chinese).

Xie, H.P., Ju, Y., Li, L.Y., 2005. Criteria for strength and structural failure of rocks based on energy dissipation and energy release principles. Chinese Journal of Rock Mechanics and Engineering 24 (17), 3003–3010 (in Chinese).

Xie, H.P., Ju, Y., Li, L.Y., Peng, R.D., 2008. Energy mechanism of deformation and failure of rock masses. Chinese Journal of Rock Mechanics and Engineering 27 (9), 1729–1740 (in Chinese).